

# THE CELT RATTLEBACK DYNAMICS WITH THE FRICTION INFLUENCE

*Institute of Mechanical Engineering Problems RAS*  
e-mail <tptovstik@mail.ru>

**1. Introduction.** The Celt stone dynamics investigation is the classical problem of the nonlinear non-holonomic dynamics of the rigid body. The convex body moves near its stable position of equilibrium on the rough horizontal plane. At the tangent point the main curvature directions of the body do not coincide with the main directions of its inertia axes. The exact system of 5th order is delivered. The various possible motions of the body near its equilibrium state are investigated analytically and numerically. Without friction the problem is conservative. One of the possible motions typical for the Celt stone is the infinite alternation of the rotation around the vertical axis in one direction, of the vibrations around the horizontal axes and of the rotation in the other direction. By the averaging method proposed by A.P.Markeev [1] and by M.Pascal [2] the problem is reduced to the system of the 3d order. The closed trajectories of the representing point lie on the surface of the 3-axes ellipsoid. In contrary to the classical approach we study the Celt stone motions with the frictions of the three types, namely the rolling friction, the rotation friction, and the air resistance. The double averaging method is used for the analytical research of the small friction influence. In the phase 3D space the representing point trajectories are not closed. The analytical and the numerical results are compared.

**2. The equations of motion.** Let the body surface near the tangent point in the reference position be paraboloid

$$z = -h + \frac{1}{2} \left( \frac{x^2}{R_1} + \frac{y^2}{R_2} \right),$$

where  $R_1$  and  $R_2$  are the main radii of curvature. The co-ordinate system  $Oxyz$  moves with the body (Fig. 1).

In the initial moment the body is deviated from the equilibrium state and it has the initial angular velocity  $\mathbf{\Omega}(0)$ . The body moves under action of the gravity and of the plane reaction. The velocity of the tangent point is equal to zero (the body do not slip).

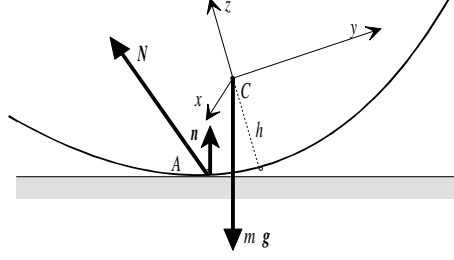


Fig. 1. The coordinate system and the external forces.

The equation of the moment balance is [3]

$$\mathbf{A}_A \cdot \dot{\boldsymbol{\Omega}} = -\boldsymbol{\Omega} \times \mathbf{A} \cdot \boldsymbol{\Omega} + m(\mathbf{g}\mathbf{n} + \boldsymbol{\Omega} \times (\boldsymbol{\Omega} \times \mathbf{r}_{AC}) - \boldsymbol{\Omega} \times \mathbf{V}_A^*) \times \mathbf{r}_{AC}. \quad (1)$$

Here  $\mathbf{A} = A_{11}\mathbf{i} \otimes \mathbf{i} + A_{22}\mathbf{j} \otimes \mathbf{j} + A_{12}(\mathbf{i} \otimes \mathbf{j} + \mathbf{j} \otimes \mathbf{i}) + A_{33}\mathbf{k} \otimes \mathbf{k}$  is the body central inertia tensor in the co-ordinate system  $x, y, z$ , the tensor  $\mathbf{A}_A = \mathbf{A} + m(\mathbf{r}_{AC}^2 \mathbf{E} - \mathbf{r}_{AC} \otimes \mathbf{r}_{AC})$  is the inertia tensor with respect to the point  $A$ , and  $m$  is the body mass. In equation (1)  $\mathbf{n}$  is the unit normal at the tangent point,  $\mathbf{r}_{AC}$  is the radius-vector of the tangent point, and  $\mathbf{V}_A^*$  is the velocity of the point  $A$  motion on the body surface. To closure system (1) we ought to add two expressions for the angular velocity through the angles of the body inclinations. Such exact expressions relations are given in [4]. Here we use its approximation.

We suppose that the angles of body inclination and its angular velocity are small. We write the projections of equation (1) and hold the terms of the second order,

$$\begin{aligned} (A_{11} + mh^2) \ddot{\vartheta}_1 + A_{12} \ddot{\vartheta}_2 + mg(R_2 - h) \vartheta_1 &= A_{01} \Omega_3 \dot{\vartheta}_2, \\ A_{12} \ddot{\vartheta}_1 + (A_{22} + mh^2) \ddot{\vartheta}_2 + mg(R_1 - h) \vartheta_2 &= -A_{02} \Omega_3 \dot{\vartheta}_1, \\ A_{33} \dot{\Omega}_3 &= (A_{11} - A_{22}) \dot{\vartheta}_1 \dot{\vartheta}_2 + A_{12} (\dot{\vartheta}_2^2 - \dot{\vartheta}_1^2) + \\ &+ mh (R_2 \vartheta_1 \ddot{\vartheta}_2 - R_1 \vartheta_2 \ddot{\vartheta}_1) + mg(R_1 - R_2) \vartheta_1 \vartheta_2, \end{aligned} \quad (2)$$

$$\begin{aligned} A_{01} &= A_{11} + A_{22} - A_{33} + mh(2h - R_1), \\ A_{02} &= A_{11} + A_{22} - A_{33} + mh(2h - R_2), \end{aligned} \quad (3)$$

where  $\Omega_3$  is the angular velocity projection on the axis  $z$ , the variables  $\vartheta_1, \vartheta_2$  are connected with the unit normal  $\mathbf{n}$  inclination by the relation

$$\mathbf{n} = -\vartheta_2 \mathbf{i} + \vartheta_1 \mathbf{j} + \left(1 - \frac{1}{2}(\vartheta_1^2 + \vartheta_2^2)\right) \mathbf{k}.$$

The first two equations (2) at  $R_1, R_2 > h$  in the first approximation describe the small vibrations, and in the second approximation the perturbing force which effect on the vibration amplitude and phase appears.

**3. The Celt effect.** After transition to the main co-ordinates the first two equations (2) accept the form

$$\begin{aligned}\ddot{\xi}_1 + \nu_1^2 \xi_1 &= \Omega_3 (f_{11} \dot{\xi}_1 + f_{12} \dot{\xi}_2), \\ \ddot{\xi}_2 + \nu_2^2 \xi_2 &= \Omega_3 (f_{21} \dot{\xi}_1 + f_{22} \dot{\xi}_2),\end{aligned}\tag{4}$$

where  $\nu_1, \nu_2$  are the eigen frequencies of the linear system,  $f_{11}, f_{12}, f_{21}, f_{22}$  are known constants.

Further we are interesting with the slowly changing amplitudes of these vibrations

$$\begin{aligned}\xi_1(t) &= p(t) \sin(\nu_1 t + \beta_1(t)), \\ \xi_2(t) &= q(t) \sin(\nu_2 t + \beta_2(t)).\end{aligned}\tag{5}$$

The third equation (2) in the first approximation gives  $\dot{\Omega}_3 = 0$ , therefore, the angular velocity around the vertical axis is the slowly changing function. By the averaging method [1], [2] system (2) is reduced to the form

$$\begin{aligned}\frac{dp}{dt} &= -a\nu_1^2 p \Omega_3, \\ \frac{dq}{dt} &= a\nu_2^2 q \Omega_3, \\ \frac{d\Omega_3}{dt} &= a/A_{33} (\nu_1^4 p^2 - \nu_2^4 q^2).\end{aligned}\tag{6}$$

By using system (6) the motion evolution may be investigated analytically. In partial it is known [5] that this system has two invariant expressions

$$\begin{aligned}\nu_1^2 p^2 + \nu_2^2 q^2 + A_{33} \Omega_3^2 &= C_1, & C_1 &= const, \\ p^\varkappa q &= C_2, & \varkappa &= \frac{\nu_2^2}{\nu_1^2}, & C_2 &= const,\end{aligned}\tag{7}$$

and the representing point trajectory in the space  $p, q, \Omega_3$  lies on the ellipsoid (Fig. 2). The part of the closed trajectory lies in the half-space  $\Omega_3 > 0$ , and the other one lies in the half-space  $\Omega_3 < 0$ . The approximate equations (6) have the periodic solution for  $p, q$  and  $\Omega_3$ ,

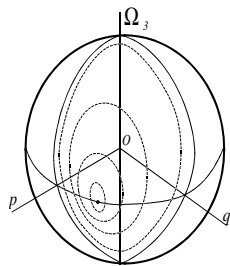


Fig. 2. The ellipsoid.

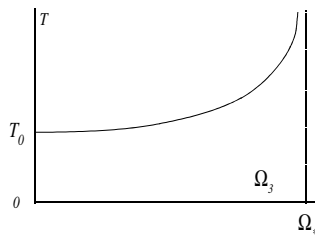


Fig 3. The period.

and it is in accordance with the numerical results for the nonzero initial data for  $p$  and  $q$ .

From relations (6) and (7) by introduce new dimensionless variables the second order equation for  $\Omega_3$  is obtained

$$\ddot{\Omega}_3 + 2 \left( \varkappa (1 - \Omega_3^2) + (1 - \varkappa) \dot{\Omega}_3 \right) \Omega_3 = 0. \quad (8)$$

This equation contains only one parameter  $\varkappa$ .

In the domain which contains in the interval  $|\Omega_3| < 1$  and depends on  $\varkappa$  the equations (7) solutions are periodic. In Fig. 3 for fixed  $\varkappa$  the typical dependence

$T(\max\{\Omega_3\})$  of the period of the representing point motion on the ellipsoid surface (Fig. 2) is presented. From Fig. 2 and Fig. 3 it is seen that the problem has periodic solution not for all values of  $\Omega_3$  and there is the critical value  $\max\{\Omega_3\} = \Omega_*(\varkappa)$  which limits the periodic solutions domain. Namely in this domain the Celt effect has place.

Near the top of the ellipsoid in Fig. 2 the amplitudes  $p$  and  $q$  are small compared with the value  $\Omega_3$ , and we study the stability of the Celt stone rotation around the main vertical inertia axis. The problem is reduced to equations in which the nonlinear terms in  $\vartheta$  are omitted. In the paper by I.S.Astapov [6] such equations are delivered and the domains of stability are found. The similar equations in our

designations are

$$\begin{aligned}
(A_{11} + mh^2) \ddot{\vartheta}_1 + A_{12} \ddot{\vartheta}_2 + mg(R_2 - h) \vartheta_1 &= \\
&= A_{01} \Omega_3 \dot{\vartheta}_2 + (A_{10} \vartheta_1 - A_{12} \vartheta_2) \Omega_3^2, \\
A_{12} \ddot{\vartheta}_1 + (A_{22} + mh^2) \ddot{\vartheta}_2 + mg(R_1 - h) \vartheta_2 &= \\
&= -A_{02} \Omega_3 \dot{\vartheta}_1 + (A_{20} \vartheta_2 - A_{12} \vartheta_1) \Omega_3^2,
\end{aligned}$$

$$A_{10} = A_{22} - A_{33} + mh(h - R_2), \quad A_{20} = A_{11} - A_{33} + mh(h - R_1).$$

For some values of the body parameters in Fig. 4 the graphics of the real parts of the characteristic polynomial are shown. For the large negative values  $\Omega_3$  the rotation around the vertical axis is stable (domain 1 in Fig. 4), and for the large positive values  $\Omega_3$  it is unstable (domain 3).

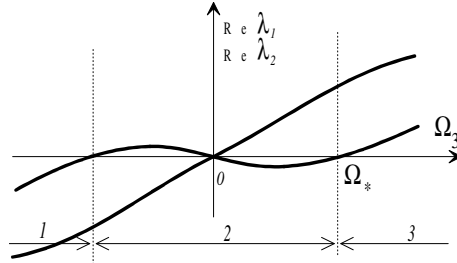


Fig. 4. The dependence of the motion regime on the angular velocity.

In domain 2 at  $|\Omega_3| < \Omega_*$  there is the interesting for us regime of vibrations where the energy transition from the rotation to the vibrations and back has place. We mark that the critical value of the angular velocity which is found by the linear theory and is shown in Fig. 4 do not coincide exactly with the maximal value  $\Omega_3$  in Fig. 2 and Fig. 3 because in equations (2) and (6) the nonlinear terms in  $\Omega_3$  are omitted.

The Celt effect is shown in Fig. 5. The results are obtained by numerical solution of the exact system. In the left side of Fig. 5 the function  $\Omega_3(t)$  variation in one period is shown. The same result may be obtained by the numerical solution of the approximate equation (8). In the right side the motion of the tangent point in the projection on the plane  $x, y$  (as the measure of the body vibrations) is shown.

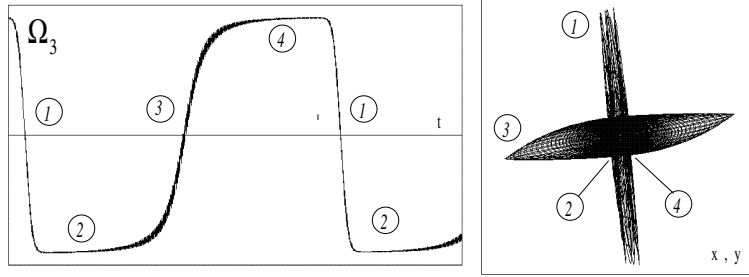


Fig. 5. The Celt effect.

In the domain 2 the rotation around the vertical axis in the negative direction with the minimal vibrations has place. At the transition to the domain 3 the sign  $\Omega_3$  changes from negative to positive, and the amplitude  $p$  is maximal (see right side of Fig. 5). In the domains 4 and 1 the body rotates in the opposite direction and the value  $q$  is larger.

**4. The friction effect.** Let the friction moment consists of three parts: of the rolling friction, of the rotation friction, and of the viscous air resistance

$$\mathbf{M}_{fr} = \mathbf{M}_{rot} + \mathbf{M}_{rol} + \mathbf{M}_{air}.$$

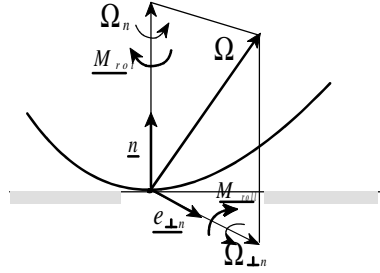


Fig. 6. the directions of the rolling friction and of the rotation friction moments.

We expand the angular velocity it two directions as it is shown in Fig. 6:

$$\boldsymbol{\Omega} = \Omega_n \mathbf{e}_n + \Omega_{pn} \mathbf{e}_{pn}, \quad \mathbf{e}_n = \pm \mathbf{n}, \quad \mathbf{e}_{pn} \cdot \mathbf{n} = 0.$$

The unit vectors  $\mathbf{e}_n$  and  $\mathbf{e}_{pn}$  directions are chosen so that  $\Omega_n > 0$ ,  $\Omega_{pn} > 0$ . If in some moment  $|\Omega_{pn}| < 10^{-7}$ , then the vector  $\mathbf{e}_{pn}$  is not introduced.

Further The rolling friction and the rotation friction moments are taken as:

$$\begin{aligned}\mathbf{M}_{roll} &= -k_{roll}\mathbf{e}_{pn}N_n, & \mathbf{M}_{rot} &= -k_{rot}\mathbf{e}_nN_n, \\ k_{rot} &= f_{rot}k_0, & k_{roll} &= f_{roll}k_0, & N_n &= \mathbf{N} \cdot \mathbf{n},\end{aligned}$$

where  $f_{rot}$ ,  $f_{roll}$  are the coefficients depending on materials,  $k_0$  is the middle surface curvature in the paraboloid top.

We take the air resistant moment as

$$\mathbf{M}_{air} = -\mathbf{B}_{air} \cdot \boldsymbol{\Omega},$$

where  $\mathbf{B}_{air}$  is the tensor depending on the body dimensions and form. Further we take  $\mathbf{B}_{air} = B_{11}\mathbf{i} \otimes \mathbf{i} + B_{22}\mathbf{j} \otimes \mathbf{j} + B_{33}\mathbf{k} \otimes \mathbf{k}$ .

The entire friction moment is

$$\mathbf{M}_{fr} = -k_{roll}N_n\mathbf{e}_{pn} - k_{rot}N_n\mathbf{e}_n - \mathbf{B}_{air} \cdot \boldsymbol{\Omega}. \quad (9)$$

After adding the external moment (9) in the right side of equation (1) equations (2) accept the form

$$\begin{aligned}(A_{11} + mh^2)\ddot{\vartheta}_1 + A_{12}\ddot{\vartheta}_2 + mg(R_2 - h)\vartheta_1 &= \\ = A_{01}\Omega_3\dot{\vartheta}_2 - mgk_{roll}\frac{\dot{\vartheta}_1}{|\dot{\boldsymbol{\theta}}|} - B_{11}\dot{\vartheta}_1 + mgk_{rot}S_0\vartheta_2, \\ A_{12}\ddot{\vartheta}_1 + (A_{22} + mh^2)\ddot{\vartheta}_2 + mg(R_1 - h)\vartheta_2 &= \\ = -A_{02}\Omega_3\dot{\vartheta}_1 - mgk_{roll}\frac{\dot{\vartheta}_2}{|\dot{\boldsymbol{\theta}}|} - B_{22}\dot{\vartheta}_2 - mgk_{rot}S_0\vartheta_1, & (10) \\ A_{33}\dot{\Omega}_3 = (A_{11} - A_{22})\dot{\vartheta}_1\dot{\vartheta}_2 + A_{12}(\dot{\vartheta}_2^2 - \dot{\vartheta}_1^2) + \\ + mh(R_2\vartheta_1\ddot{\vartheta}_2 - R_1\vartheta_2\ddot{\vartheta}_1) + mg(R_1 - R_2)\vartheta_1\vartheta_2 - \\ - mgk_{rot}S_0 - B_{33}\Omega_3 - mgk_{roll}\frac{\vartheta_2\dot{\vartheta}_1 - \vartheta_1\dot{\vartheta}_2}{|\dot{\boldsymbol{\theta}}|}.\end{aligned}$$

Here constants  $A_{01}$ ,  $A_{02}$  are given by relations (3) again,

$$S_0 = \mathbf{sign}(\Omega_n), \quad \Omega_n = \Omega_3 + o(\vartheta), \quad \dot{\boldsymbol{\theta}} = \dot{\vartheta}_1\mathbf{i} + \dot{\vartheta}_2\mathbf{j}.$$

From these equations it is seen that the viscous friction coefficient is multiplied on the small angular velocities of inclination in the first

two equations and on the small angular velocity around the vertical axis in the third equation. The rotation friction  $k_{rot}$  acts the brake effect in the third equation, and in the first two equations it lead to the frequencies changing. On the contrary the rolling friction leads to the vibrations dissipation in the first two equations, and in the third equation the coefficient  $k_{roll}$  is multiplied on the small value  $(\vartheta_2\dot{\vartheta}_1 - \vartheta_1\dot{\vartheta}_2) / \sqrt{\dot{\vartheta}_1^2 + \dot{\vartheta}_2^2}$  which may be as positive so negative. We neglect in analytical researches the small influence of the rotation friction in the first two equations and the rolling friction in the third equation.

**5. The friction effects. The numerical results.** The various types of friction effect for various initial conditions is studied numerically. One of the numerical effects may be well described by the approximate system (10). If the initial conditions for the angles of inclination and its velocity are small, but the angular velocity  $\Omega_3(0)$  is not small and lies in the Celt effect zone (Fig. 4), then the body vibrations may be absent due to the damping effect of the rolling friction, which do not depend on the angles of inclination and may be larger than the rest terms in the first two equations.

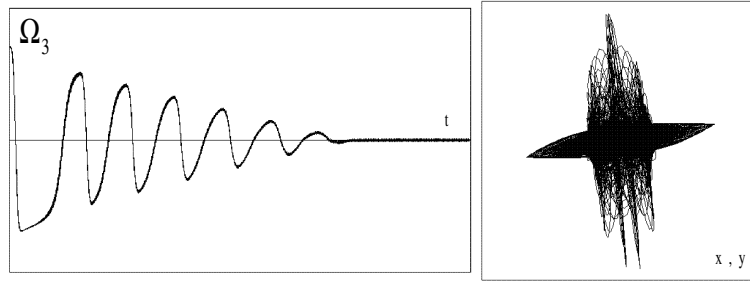


Fig. 7. The rotation friction effect.

Fig. 7 and Fig. 8 illustrate the friction effect during some periods. The rotation friction mainly acts on the angular velocity  $\Omega_3$  and fully it does not dump out the vibrations. The rolling friction and the rotation friction at first lead to decrease the  $\Omega_3$  period and then the period increase. The viscous resistance also leads to the period increase.

**6. The friction effects. The analytical research.** By the averaging method system (10) is transformed to the approximate one similar to

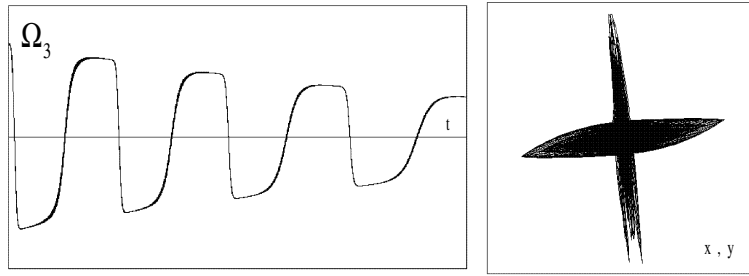


Fig. 8. The effect of the viscous air resistance.

(6)

$$\begin{aligned}
 \frac{dp}{dt} &= -a\nu_1^2 p \Omega_3 - k_{air1} p - k_{roll} I_1(p, q), \\
 \frac{dq}{dt} &= a\nu_2^2 q \Omega_3 - k_{air2} q - k_{roll} I_2(p, q), \\
 \frac{d\Omega_3}{dt} &= \frac{a}{A_{33}} (\nu_1^4 p^2 - \nu_2^4 q^2) - k_{air3} \Omega_3 - k_{rot} \frac{\Omega_3}{|\Omega_3|},
 \end{aligned} \tag{11}$$

where

$$\begin{aligned}
 I_1 &= \lim_{T_0 \rightarrow \infty} \frac{1}{T_0} \int_0^{T_0} \frac{\dot{\vartheta}_1 + \alpha_1 \dot{\vartheta}_2}{\nu_1 a_1 |\dot{\theta}|} \cos(\nu_1 t + \beta_1) dt, \\
 I_2 &= \lim_{T_0 \rightarrow \infty} \frac{1}{T_0} \int_0^{T_0} \frac{\alpha_2 \dot{\vartheta}_1 + \dot{\vartheta}_2}{\nu_2 a_2 |\dot{\theta}|} \cos(\nu_2 t + \beta_2) dt.
 \end{aligned} \tag{12}$$

In this case the values  $C_1$  and  $C_2$  in relation (7) are slowly changing functions of time.

Найдя производные по времени от этих величин и вторично воспользовавшись методом осреднения [7], находим период для  $\Omega_3$  в зависимости от времени. Траектории изображающей точки на эллипсоиде (рис. 2) становятся незамкнутыми.

#### References

- [1] Markeev A. P. On the rigid body dynamics on the absolutely rough plane // J. Appl. Maths Mechs. 1983. V.47, no 4. Pp. 575–582.
- [2] Pascal M. Asymptotic solution of equations of the Celt stone motion // J. Appl. Maths Mechs. 1983. V.46, no 2. Pp. 321–329.
- [3] Zhilin P.A. A New Approach to the Analysis of Free Rotations of Rigid Bodies // ZAMM – Z. angew. Math. Mech. 76 (1996), т 4, pp. 187–204.

- [4] Tovstik T.P. Analytical research of the Celt stone dynamics // XXXI Summer School. Advanced Problems in Mechanics. APM 2003, St.Petersburg.
- [5] *Markeev A.P.* Dynamics of the body being contiguous to a rigid surface. Moscow, Nauka, 1992., 336 p.
- [6] *Astapov I.S.* On the stability of the Celt stone rotation // Bull Moscow Univ. Ser.1, Math., mechan. 1980. N 2. Pp. 97–100.
- [7] Tovstik T.P. On the influence of friction on the Celt rattleback motion // XXXIII Summer School. Advanced Problems in Mechanics. APM 2005, St.Petersburg.